Equatorial Shelf Waves on an Exponential Shelf Profile

LAWRENCE A. MYSAK[1]

National Center for Atmospheric Research,[2] Boulder, Colo. 80307

(Manuscript received 10 October 1977)

ABSTRACT

The theory of barotropic nondivergent waves trapped on an exponential shelf lying on an equatorial β-plane is presented. The bottom contours are parallel to the equator so that phase propagation is either eastward or westward, according to the following general rule: when the shelf region is entirely in the Northern (Southern) Hemisphere the shallow water is to the right (left) of the direction of the phase velocity. When both the shelf and deep sea regions are located in the same hemisphere (case 1), the results concerning the dispersion curves and eigenfunctions are qualitatively similar to those obtained by Buchwald and Adams (1968) for shelf waves on a mid-latitude exponential shelf on an f-plane. However, when the shelf region is on one side of the equator and the deep sea region extends across the equator (case 2), the dispersion curves and eigenfunctions are quire different. In case 2 the dispersion curve for each trapped mode has a long-wave cutoff. However, the cutoff for each mode generally does not preclude the existence of a zero group velocity at an intermediate wavelength, a phenomenon which always occurs in case 1. In case 2 the range of oscillation for each eigenfunction is generally much larger than that of the corresponding eigenfunction in case 1. Finally, when the shelf region straddles the equator (case 3), both westward and eastward propagating modes may exist. Further, one set of these modes has a long-wave cutoff (e.g., if the coast is in the Southern Hemisphere with deep water to the north, the westward propagating modes have a long-wave cutoff). In case 3 the oscillations of each eigenfunction tend to be concentrated near the shelf edge.

The theory is applied to the Gulf of Guinea, where a 0.07 cycle per day (cpd) oscillation in the sea surface temperature has been observed to propagate westward along the Ghana-Ivory coast. It is shown that this signal may be due to the presence of a fundamental mode shelf wave of the type discussed in this paper.

1. Introduction

A theory of barotropic, nondivergent, zonally propagating waves on an equatorial beta plane with topography has recently been presented by Mysak (1978, hereafter referred to as M). In M the depth profile H is assumed to be a function only of y, the northward coordinate, and solutions are given for long-period trapped waves on a number of profiles that describe different types of escarpment and continental shelf/slope regions. However, in M the trapping of long-period waves on the exponential shelf profile, first introduced into the literature by Buchwald and Adams (1968), was not discussed. The purpose of this paper is to fill this gap in the literature. Also, because the Buchwald-Adams profile has been extensively used in the *midlatitude* shelf wave literature, it was felt that a separate study should be made of *equatorial* shelf waves that propagate on this profile.

In Section 2 the boundary value problem for the amplitude of nondivergent, equatorial trapped waves on an arbitrary depth profile $H(y)$ is presented. In Section 3 the problem for the exponential profile is then formulated. In Section 4 a number of qualitative results concerning the phase and group velocities are proved and bounds for the eigenfrequencies are established. Next, in Section 5, the implicit dispersion relation (involving Bessel functions of fractional order) is derived. In Section 6, the dispersion curves for the first few modes along with the profiles of the corresponding eigenfunctions are shown. Finally, in Section 7 the theory is applied to the Gulf of Guinea, West Africa, in an attempt to explain the presence of a long-period westward propagating signal in the sea surface temperature.

2. Boundary value problem for the wave amplitude

Let $\Psi(x,y,t)$ denote the mass transport streamfunction; then the eastward (x) and northward (y) velocity components are given by

$$u = -\Psi_y/H \quad \text{and} \quad v = \Psi_x/H, \tag{2.1}$$

respectively. Further, if Ψ has the travelling wave form

[1] Permanent affiliation: Department of Mathematics and Institute of Oceanography, The University of British Columbia, Vancouver, B. C., Canada V6T 1W5.

[2] The National Center for Atmospheric Research is sponsored by the National Science Foundation.

0022-3670/78/0458-0467$05.00

$$\Psi = \psi(y)e^{i(kx-\omega t)}, \quad k > 0, \tag{2.2}$$

then the linearized equations for barotropic, nondivergent, unforced motions on an equatorial beta plane with depth profile $H(y)$ imply that $\psi(y)$ satisfies [cf. Eq. (2.6) in M]

$$(\psi'/H)' - [k^2/H + (k\beta/\omega)(y/H)']\psi = 0, \tag{2.3}$$

where the prime indicates d/dy and $\beta = 2\Omega_E/R$, Ω_E and R being the earth's angular velocity and radius, respectively.

Let us first suppose that the domain of (2.3) is $y_c \leq y \leq \infty$ (deep water to the north). To ensure that Hu be zero at the coast and that the waves be trapped against the shelf region, we impose the boundary conditions

$$\psi = 0 \quad \text{at} \quad y = y_c, \tag{2.4}$$

$$\psi \to 0 \quad \text{as} \quad y \to \infty. \tag{2.5}$$

If H or H' is discontinuous at $y = y_e \in (y_c,\infty)$, then the following jump conditions must be imposed [cf. (2.9) and (2.10) in M where a derivation of these conditions is given]:

$$[\psi] = 0, \quad \text{at} \quad y = y_e, \tag{2.6}$$

$$[\psi'/H] - (\beta k y_e/\omega)\psi(y_e)[1/H] = 0, \quad \text{at} \quad y = y_e. \tag{2.7}$$

We now consider a class of depth profiles of the form

$$H(y) = \begin{cases} H_s(y), & y_c \leq y \leq y_e \text{ (shelf region)} \\ H_d, & y_e \leq y \leq \infty \text{ (deep sea region)} \end{cases} \tag{2.8}$$

where $H_s(y_e) = H_d$ = constant. Then the solution of (2.3) for $y_e \leq y \leq \infty$ subject to the condition (2.5) is

$$\psi_d = Ae^{-Ky}, \tag{2.9}$$

where $K = (k^2 + k\beta/\omega)^{1/2} > 0$. Let ψ_s denote the solution of (2.3) for $y_c \leq y \leq y_e$. Then the application of (2.6) and (2.7) to ψ_d and ψ_s gives

$$\psi_s' + K\psi_s = 0 \quad \text{at} \quad y = y_e. \tag{2.10}$$

Thus for profiles of the form (2.8), the boundary value problem for ψ reduces to one for ψ_s alone on the finite interval $y_c \leq y \leq y_e$ with the endpoint conditions being (2.4) and (2.10).

If the domain of (2.3) is $-\infty \leq y \leq y_c$ (deep water to the south), then in place of (2.5) we have

$$\psi \to 0 \quad \text{as} \quad y \to -\infty. \tag{2.5}'$$

Further, for profiles of the form

$$H(y) = \begin{cases} H_s(y), & y_e \leq y \leq y_c \\ H_d, & -\infty \leq y \leq y_e \end{cases} \tag{2.8}'$$

where again $H_s(y_e) = H_d$ = constant, it follows that the boundary condition (2.10) changes to

$$\psi_s' - K\psi_s = 0 \quad \text{at} \quad y = y_e. \tag{2.10}'$$

3. The exponential shelf profile

The exponential shelf profile introduced into the literature by Buchwald and Adams (1968, hereafter referred to as BA) falls into the depth profile class (2.8) discussed in the previous section. However, since we are dealing here with an equatorial beta plane rather than a mid-latitude f-plane (as in BA) care must be taken to distinguish between the cases 1) deep water to the north and 2) deep water to the south. In the first case the BA profile takes the form

$$H(y) = \begin{cases} H_0e^{2by}, & y_c = y_e - l \leq y \leq y_e \\ H_d, & y_e \leq y \leq \infty \end{cases} \tag{3.1}$$

where $b > 0$, $l > 0$ and $0 < H_d = H_0e^{2by_e}$; here y_e is the position of the shelf edge and l the width of the shelf. In the second case

$$H(y) = \begin{cases} H_0e^{2by}, & y_e \leq y \leq y_e + l = y_c \\ H_d, & -\infty \leq y \leq y_e \end{cases} \tag{3.1}'$$

where here $b < 0$.

We first consider the case $b > 0$. The substitution of (3.1) into (2.3) gives

$$\psi'' - 2b\psi' - [K^2 - (2bk\beta/\omega)y]\psi = 0, \quad y_e - l \leq y \leq y_e. \tag{3.2}$$

The appropriate boundary conditions are (2.4) and (2.10). Let us now introduce the normalized variable

$$\eta = (y - y_e + l)/l = (y - y_c)/l. \tag{3.3}$$

Then (3.2) becomes

$$\frac{d^2\psi}{d\eta^2} - 2B\frac{d\psi}{d\eta} - [\chi^2 - (\eta + \gamma - 1)2B\kappa/\Omega]\psi = 0, \quad 0 \leq \eta \leq 1, \tag{3.4}$$

where

$$\left.\begin{aligned} B &= bl > 0 \\ \gamma &= y_e/l \\ \kappa &= kl > 0 \\ \Omega &= \omega/\beta l \\ \chi &= (\kappa^2 + \kappa/\Omega)^{1/2} > 0 \end{aligned}\right\}. \tag{3.5}$$

The boundary conditions transform into

$$\psi = 0 \quad \text{at} \quad \eta = 0, \tag{3.6}$$

$$\frac{d\psi}{d\eta} + \chi\psi = 0 \quad \text{at} \quad \eta = 1. \tag{3.7}$$

In (3.5) κ and Ω are the nondimensional wave-

number and frequency, respectively; B and γ respectively characterize the curvature of the shelf and the location of the shelf relative to the equator. For $B \ll 1$ the shelf profile is approximately linear, whereas for $B \gg 1$ the shelf is fairly flat near the coast and then drops off rapidly as $\eta \to 1$. In typical ocean shelf/slope regions, $B \geq O(1)$. There are three important parameter ranges for γ: $1 < \gamma$, shelf is north of the equator; $0 < \gamma < 1$, shelf straddles the equator; $\gamma < 0$, shelf is south of the equator.

We now consider the case $b < 0$ (deep water to the south). The substitution of (3.1)′ into (2.3) again gives (3.2), with the domain now being $y_e \leq y \leq y_e + l = y_c$. The appropriate boundary conditions are now (2.4) and (2.10)′. Next, if we put

$$\eta' = (y_e + l - y)/l = (y_c - y)/l, \tag{3.8}$$

we obtain the boundary value problem

$$\frac{d^2\psi}{d\eta'^2} - 2B'\frac{d\psi}{d\eta'} - [\chi^2 - (\eta' - \gamma - 1)2B'\kappa/\Omega]\psi = 0, \quad 0 \leq \eta' \leq 1 \tag{3.9}$$

$$\psi = 0 \quad \text{at} \quad \eta' = 0, \tag{3.10}$$

$$\frac{d\psi}{d\eta'} + \chi\psi = 0 \quad \text{at} \quad \eta' = 1, \tag{3.11}$$

where $B' = -bl > 0$, the other parameters being the same as in (3.5). While B' has the same meaning as before, it now follows that when $0 < \gamma$, the shelf is north of the equator; when $-1 < \gamma < 0$, the shelf straddles the equator; and when $\gamma < -1$, the shelf is south of the equator.

Comparison of the system (3.9)–(3.11) with that for $b > 0$ reveals that the solution of (3.9)–(3.11) for $B' = B_0$ and $\gamma = \gamma_0$ is identical to that of (3.4)–(3.7) for $B = B_0$ and $\gamma = -\gamma_0$. Therefore, henceforth we shall only focus our attention on the system (3.4)–(3.7), with γ taking on both positive and negative values.

If we make the substitution

$$\psi = e^{B\eta}\phi \tag{3.12}$$

into (3.4), (3.6) and (3.7), we obtain the following system:

$$\frac{d^2\phi}{d\eta^2} + [(\gamma - 1)2B\kappa/\Omega - \chi^2 - B^2 + (2B\kappa/\Omega)\eta]\phi = 0, \quad 0 \leq \eta \leq 1, \tag{3.13}$$

$$\phi = 0 \quad \text{at} \quad \eta = 0, \tag{3.14}$$

$$\frac{d\phi}{d\eta} + (\chi + B)\phi = 0 \quad \text{at} \quad \eta = 1. \tag{3.15}$$

The canonical form of (3.13) can now be identified as a variant of Bessel's equation (see Section 5) and can also be readily used to prove some general results concerning the signature of the phase velocity $C = \Omega/\kappa$ and the group velocity $C_g = \partial\Omega/\partial\kappa$ (see Section 4).

4. Qualitative results

If we multiply (3.13) by ϕ, integrate with respect to η over (0,1) and then invoke (3.14) and (3.15), we find

$$C = \frac{\Omega}{\kappa} = \frac{2B\int_0^1 \eta\phi^2 d\eta + \Delta\int_0^1 \phi^2 d\eta}{\int_0^1 [(\kappa^2 + B^2)\phi^2 + \phi'^2]d\eta + E}, \tag{4.1}$$

where $\Delta = (\gamma - 1)2B - 1, E = [B + (\kappa_2 + 1/C)^{1/2}]\phi^2(1)$. We recall that for trapped waves, $(\kappa^2 + 1/C)^{1/2} > 0$, which must hold for either positive or negative C. Therefore the signature of C is determined by the signature of the numerator in the right side of (4.1) since the denominator there is positive. Since the first term in the numerator is positive definite, we have

THEOREM 1. If $\Delta = (\gamma - 1)2B - 1 > 0$, then the phase speed $C > 0$ (eastward phase propagation with shallow water to the right).

The condition $\Delta > 0$ can be written as

$$\gamma > 1 + 1/2B. \tag{4.2}$$

Recalling that $\gamma > 1$ corresponds to the shelf being strictly north of the equator, we see that (4.2) is satisfied for $B \gg 1$ (sharp drop at shelf edge) when the coast is just north of the equator. However, when $B \ll 1$ (a linear shelf), the coast must be sufficiently far north of the equator for (4.2) to hold. Hereafter we shall refer to this topographic configuration as case 1.

We now suppose that $\Delta > 0$ and hence by Theorem 1, that $C > 0$, which of course implies that

$$\Omega > 0 \tag{4.3}$$

since $\kappa > 0$. Further, let N and D denote respectively the numerator and denominator of the right side of (4.1). It follows that

$$\mathrm{N} < (2B + \Delta)\int_0^1 \phi^2 d\eta, \tag{4.4}$$

$$\mathrm{D} > (\kappa^2 + B^2)\int_0^1 \phi^2 d\eta. \tag{4.5}$$

Using (4.4) and (4.5), Eq. (4.1) thus gives

$$\frac{\Omega}{\kappa} = \frac{\mathrm{N}}{\mathrm{D}} < \frac{2B + \Delta}{\kappa^2 + B^2},$$

which implies

$$\Omega < (2B + \Delta)\kappa/(\kappa^2 + B^2). \tag{4.6}$$

Combining (4.3) and (4.6), we finally obtain

$$0 < \Omega < (2B + \Delta)\kappa/(\kappa^2 + B^2) \tag{4.7}$$

for $\Delta > 0 (\gamma > 1 + 1/2B)$. Thus $\Omega \downarrow 0$ as $\kappa \downarrow 0$ and as $\kappa \uparrow \infty$. Hence assuming that $\Omega(\kappa)$ is continuous, we have

THEOREM 2. If $\Delta > 0$, then $C_g = \partial\Omega/\partial\kappa = 0$ for some value of $\kappa = \kappa_1$, say, where $0 < \kappa_1 < \infty$.

The discovery of the existence of a zero group velocity for shelf waves on the midlatitude BA shelf was one of the highlights in BA's paper. Thus it is interesting to see that the same result also carries over to equatorial shelf waves on the BA shelf, provided the coast is sufficiently far north of the equator so that the criterion (4.2) holds. As a consequence of Theorem 2 it follows that for $\kappa < \kappa_1$ ("long" waves) the energy and phase both propagate eastward, whereas for $\kappa > \kappa_1$ ("short" waves) the energy propagates in the opposite sense to the phase.

We now establish bounds for the frequencies when $\Delta < 0$. We first consider the case $\Delta < -2B$, which implies that

$$\gamma < 1/2B. \tag{4.8}$$

Since $B \geq O(1)$ in practice (see Section 7), this case generally corresponds to the shelf being in the Southern Hemisphere with the deep water to the north. We shall refer to this topographic configuration as case 2. Now, since $B > 0$, we have

$$\Delta \int_0^1 \phi^2 d\eta < 2B \int_0^1 \eta\phi^2 d\eta + \Delta \int_0^1 \phi^2 d\eta < (2B + \Delta) \int_0^1 \phi^2 d\eta. \tag{4.9}$$

Further, we recall that for trapped waves, $\kappa^2 + \kappa/\Omega > 0$, which holds (for $\kappa > 0$) provided $\Omega > 0$ or $\Omega < -1/\kappa$, i.e., provided Ω does not lie in the closed interval $[-1/\kappa, 0]$:

$$\Omega \notin [-1/\kappa, 0]. \tag{4.10}$$

Under the restriction (4.10), the denominator D of the right side of (4.1) is positive. Therefore, on dividing (4.9) by D and using (4.1) we obtain

$$\frac{\Delta \int_0^1 \phi^2 d\eta}{D} < \frac{\Omega}{\kappa} < \frac{(2B + \Delta) \int_0^1 \phi^2 d\eta}{D}. \tag{4.11}$$

Therefore for case 2, in which $2B + \Delta < 0$, the right-hand inequality of (4.11) implies that the frequency is always negative. But since (4.10) must also hold, the following in equality is deduced:

$$\Omega < -1/\kappa. \tag{4.12}$$

Now in view of (4.5) and the fact that $\Delta < 0$ for case 2, (4.11) also implies that

$$\frac{\Omega}{\kappa} > \frac{\Delta \int_0^1 \phi^2 d\eta}{D} > \frac{\Delta}{\kappa^2 + B^2}. \tag{4.13}$$

Combining (4.12) and (4.13), we thus find

$$\Delta\kappa/(\kappa^2 + B^2) < \Omega < -1/\kappa \tag{4.14}$$

for case 2, $\Delta < -2B (\gamma < 1/2B)$.

Finally, we consider the intermediate case $-2B < \Delta < 0$, or equivalently,

$$1/2B < \gamma < 1 + 1/2B. \tag{4.15}$$

Generally speaking, this corresponds to the situation in which the shelf straddles the equator with deep water to the north; it will be referred to as case 3. For this case we note that while $\Delta < 0$, $2B + \Delta > 0$; therefore, (4.11) implies that both negative and positive frequencies are possible. However, in view of (4.10), Eq. (4.11) must be broken up into two parts:

$$\frac{\Delta \int_0^1 \phi^2 d\eta}{D} < \frac{\Omega}{\kappa} < -\frac{1}{\kappa^2}$$

or

$$0 < \frac{\Omega}{\kappa} < \frac{(2B + \Delta) \int_0^1 \phi^2 d\eta}{D}.$$

Again using (4.5), we hence obtain

$$\Delta\kappa/(\kappa^2 + B^2) < \Omega < -1/\kappa$$

or

$$0 < \Omega < (2B + \Delta)\kappa/(\kappa^2 + B^2) \tag{4.16}$$

for case 3, $-2B < \Delta < 0$ $(1/2B < \gamma < 1 + 1/2B)$.

The inequalities (4.7), (4.14) and (4.16) giving upper and lower bounds for the frequencies were of considerable help in computing the dispersion curves shown in Section 6. For a prescribed pair of values of B and γ, the corresponding value of Δ was computed, which in turn specified which type of topographic configuration was being considered. The appropriate frequency bounds were then incorporated into the program, which thus ensured that no modes were missed in the search for the roots of the implicit dispersion relation $F(\Omega,\kappa) = 0$.

5. The dispersion relation and eigenfunctions

We now derive the solution of the system (3.13)–(3.15) in terms of Bessel functions. If $\Omega > 0$ then

the coefficient of η in (3.13) is positive. Therefore when $\Omega > 0$, we let [cf. (3.13)]

$$\lambda^2\mu = \Delta\kappa/\Omega - \kappa^2 - B^2 + \lambda^2\eta, \tag{5.1}$$

where $\lambda = (2B\kappa/\Omega)^{1/2} > 0$. Then the system (3.13)–(3.15) becomes

$$\frac{d^2\phi}{d\mu^2} + \lambda^2\mu\phi = 0, \quad \mu_0 \leq \mu \leq \mu_1, \tag{5.2}$$

$$\phi = 0 \quad \text{at} \quad \mu = \mu_0, \tag{5.3}$$

$$\frac{d\phi}{d\mu} + (\chi + B)\phi = 0 \quad \text{at} \quad \mu = \mu_1, \tag{5.4}$$

where

$$\mu_0 = (\Delta\kappa/\Omega - \kappa^2 - B^2)/\lambda^2, \tag{5.5}$$

$$\mu_1 = \mu_0 + 1. \tag{5.6}$$

The general solution of (5.2) can be written as (Abramowitz and Stegun, 1965, p. 362)

$$\phi = A_1\mu^{1/2}J_{1/3}(\tfrac{2}{3}\lambda\mu^{3/2}) + A_2\mu^{1/2}J_{-1/3}(\tfrac{2}{3}\lambda\mu^{3/2}). \tag{5.7}$$

Alternatively, since (5.2) is a simple variant of Airy's equation (see Abramowitz and Stegun, 1965, p. 446), the solution can also be written in the form

$$\phi = A_1\mathrm{Ai}(-\lambda^{2/3}\mu) + A_2\mathrm{Bi}(-\lambda^{2/3}\mu), \tag{5.7}'$$

where Ai and Bi are the Airy functions. These are entire functions of μ which are oscillatory if $\mu > 0$ and are of exponential character if $\mu < 0$. It can be shown that $\mu^{1/2}J_{1/3}$ and $\mu^{1/2}J_{-1/3}$ are also entire functions of μ with a similar behavior when $\mu > 0$ and $\mu < 0$. However, when $\mu < 0$ (which can occur when say $\mu_0 < 0$), the Bessel functions $J_{\pm 1/3}$ become proportional to the modified Bessel functions $I_{\pm 1/3}$ [see Eq. (5.12)]. The dispersion relation is obtained from the conditions (5.3) and (5.4). Substituting (5.7) into these equations gives

$$\mu_0^{1/2}\{A_1J_{1/3}^{(0)} + A_2J_{-1/3}^{(0)}\} = 0, \tag{5.8}$$

$$\mu_1^{1/2}\{A_1[(\chi + B)J_{1/3}^{(1)} + \lambda\mu_1^{1/2}J_{-2/3}^{(1)}] + A_2[(\chi + B)J_{-1/3}^{(1)} - \lambda\mu_1^{1/2}J_{2/3}^{(1)}]\} = 0, \tag{5.9}$$

where $J_\nu^{(0)} = J_\nu(\tfrac{2}{3}\lambda\mu_0^{3/2})$ and similarly for $J_\nu^{(1)}$. In arriving at (5.9) we have used the well-known Bessel function recurrence relations to eliminate the derivatives of $J_{\pm 1/3}^{(1)}$ that arise in (5.4) (Abramowitz and Stegun, 1965 p. 361). For a nontrivial solution for A_1 and A_2, we require that the determinant of coefficients in (5.8) and (5.9) be zero, i.e.,

$$(\mu_0\mu_1)^{1/2}\{J_{1/3}^{(0)}[(\chi + B)J_{-1/3}^{(1)} - \lambda\mu_1^{1/2}J_{2/3}^{(1)}] - J_{-1/3}^{(0)}[(\chi + B)J_{1/3}^{(1)} + \lambda\mu_1^{1/2}J_{-2/3}^{(1)}]\} = 0. \tag{5.10}$$

For given values of B and γ, Eq. (5.10) represents an implicit form of the dispersion relation $\Omega = \Omega(\kappa)$. The presence of the factor $(\mu_0\mu_1)^{1/2}$ in (5.10) ensures that each term is analytic in both μ_0 and μ_1. Since the Bessel functions are oscillatory in character, there will be an infinity of solutions (eigenfrequencies) $\Omega = \Omega_n(\kappa)$, $n = 0, 1, 2, 3, \ldots$ of (5.10). Since $\Omega > 0$, we shall adopt the ordering $\Omega_0 > \Omega_1 > \ldots > 0$ for these eigenfrequencies. The eigenfunction in terms of the mass transport streamfunction [see (3.12)] for the nth mode is given by

$$\psi_n(\mu) = e^{B\eta}\mu^{1/2}\left[J_{-1/3}(\tfrac{2}{3}\lambda\mu^{3/2}) - \frac{J_{-1/3}^{(0)}}{J_{1/3}^{(0)}}J_{1/3}(\tfrac{2}{3}\lambda\mu^{3/2})\right], \quad \mu_0 \leq \mu \leq \mu_0 + 1, \tag{5.11}$$

where $\eta(\mu) = (\lambda^2\mu + \kappa^2 + B^2 - \Delta\kappa/\Omega_n)/\lambda^2$ and it is understood that in λ and μ_0, $\Omega = \Omega_n$. In arriving at (5.11) we have used (5.8) to eliminate A_1 in (5.7) and then set $A_2 = 1$.

When $\Omega < 0$, the coefficient of η in (3.13) is negative and the solution of this equation can be written as

$$\phi = A_1\mu'^{1/2}I_{1/3}(\tfrac{2}{3}\lambda'\mu'^{3/2}) + A_2\mu'^{1/2}I_{-1/3}(\tfrac{2}{3}\lambda'\mu'^{3/2}), \quad \mu_0' \leq \mu' \leq \mu_1' = \mu_0' + 1, \tag{5.12}$$

where

$$\lambda' = (-2B\kappa/\Omega)^{1/2} > 0,$$

$$\lambda'^2\mu' = \kappa^2 + B^2 - \Delta\kappa/\Omega + \lambda'^2\eta, \tag{5.13}$$

$$\mu_0' = (\kappa^2 + B^2 - \Delta\kappa/\Omega)/\lambda'^2.$$

Alternatively, when $\Omega < 0$ the solution of (3.13) can be written as

$$\phi = A_1\mathrm{Ai}(\lambda'^{2/3}\mu') + A_2\mathrm{Bi}(\lambda'^{2/3}\mu'). \tag{5.12}'$$

It is again important to note that even when $\Omega < 0$, μ_0' can be negative (since $\Delta < 0$) and therefore $\mu' < 0$ for part of the range of μ'. That is, the solution is oscillatory and the modified Bessel functions transform into the standard Bessel functions. Proceeding as in the case $\Omega > 0$, we find that the implicit dispersion relation for $\Omega < 0$ is given by

$$(\mu_0'\mu_1')^{1/2}\{I_{1/3}^{(0)}[(\chi + B)I_{-1/3}^{(1)} + \lambda'\mu_1'^{1/2}I_{2/3}^{(1)}] - I_{-1/3}^{(0)}[(\chi + B)I_{1/3}^{(1)} + \lambda'\mu_1'^{1/2}I_{-2/3}^{(1)}]\} = 0, \tag{5.15}$$

where $I_\nu^{(0)} = I_\nu(\tfrac{2}{3}\lambda'\mu_0'^{2/3})$ and similarly for $I_\nu^{(1)}$. For a given pair of B, γ values we shall order the roots $\Omega_n(\kappa)$ of (5.15) as follows: $\Omega_0 < \Omega_1 < \Omega_2 < \ldots < 0$. The mass transport eigenfunction corresponding to the eigenfrequency Ω_n is given by

$$\psi_n = e^{B\eta}\mu'^{1/2}\left[I_{-1/3}(\tfrac{2}{3}\lambda'\mu'^{3/2}) - \frac{I_{-1/3}^{(0)}}{I_{1/3}^{(0)}}I_{1/3}(\tfrac{2}{3}\lambda'\mu'^{3/2})\right], \quad \mu_0' \leq \mu' \leq \mu_0' + 1, \tag{5.16}$$

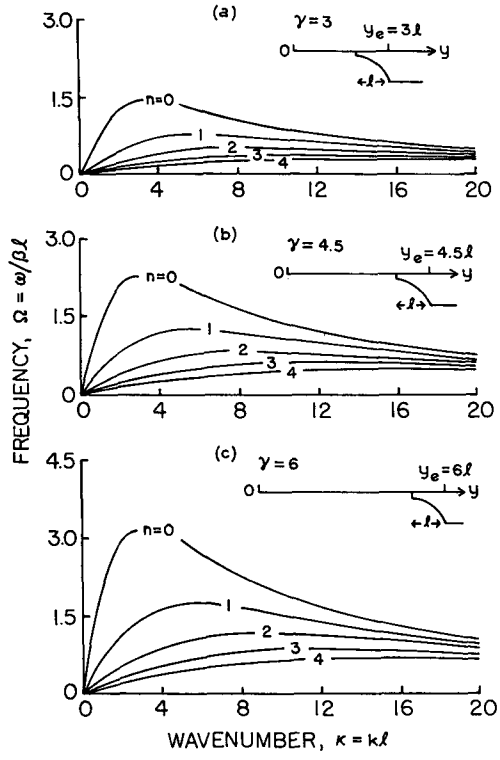

FIG. 1. The dispersion curves of the first five modes ($n = 0, 1, 2, 3, 4$) computed from Eq. (5.10) for $B = bl = 2(b > 0)$ and $\gamma = 3, 4, 5$ and 6. The parameter $\gamma = y_e/l > 0$ is a measure of the distance of shelf break (at $y = y_e$) northward from the equator (see insets). In view of the comments prior to (3.12), these curves also apply to the cases $B = -2$ ($b < 0$) and $\gamma = -3.0, -4.5, -6.0$ (shelf in Southern Hemisphere with deep water to the south).

where $\eta(\mu') = [\lambda'^2\mu' + \Delta\kappa/\Omega_n(\kappa) - \kappa^2 - B^2]/\lambda'^2$ and $\Omega_n(\kappa)$ is the solution of (5.15).

6. Numerical results

Dispersion curves and the corresponding eigenfunctions were computed from the solutions presented in Section 5. Values of B and γ were chosen so that all three types of topographic configurations defined in Section 4 were represented: 1) $\gamma > 1 + 1/2B(\Delta > 0)$; 2) $\gamma < 1/2B(\Delta < -2B)$; 3) $1/2B < \gamma < 1 + 1/2B(-2B < \Delta < 0)$. Figs. 1–3, Figs. 4 and 5, and Figs. 6 and 7 respectively show representative solutions for these three cases.

The dispersion curves Ω vs κ of the first five modes for positive values of B and γ such that $\gamma > 1 + 1/2B$ (case 1) are shown in Figs. 1 and 2. As expected all the roots are positive, implying eastward phase propagation. In accordance with Theorem 2, we note from Figs. 1 and 2 that each mode has a zero group velocity at an intermediate wavenumber. Further, at long wavelengths (small κ) the waves are nondispersive, and as $\kappa \to \infty$, $\Omega \to 0$. These curves are thus qualitatively very similar to those for a mid-latitude exponential shelf on an f-plane (cf. Fig. 4 in BA). In particular, we note that for a fixed shelf width l, the frequency ω at a given wavenumber increases as either y_e increases or b increases. This is to say, the phase speed is increased when the shelf is located further north of the equator or the shelf curvature is increased.

Fig. 3 shows the eigenfunctions ψ_n for a fixed pair of positive B, γ values and for an intermediate value of κ; the corresponding eigenfrequencies are obtained from Fig. 2c. For $n \geq 1$, these curves are oscillatory in character, with the nth mode eigenfunction having n zero crossings. The lowest mode eigenfunction ψ_0 does not have a zero crossing, however, and consists of both an oscillatory part ($0.7 < \eta < 1$) and a monotonic part ($0 < \eta < 0.7$). This is because in this case $\mu_0 < 0 < \mu_1$ and hence μ in the solution (5.7) or (5.7)′ takes on both negative and positive values.

Fig. 4 shows the dispersion curves for the case $B = 3$ and three values of $\gamma < 0$, chosen so that $\gamma < 1/2B$ (case 2). Now the waves all propagate westward, but as in case 1 each mode has a zero group velocity at an intermediate value of κ. The presence of the long-wave cutoff at $\Omega = -1/\kappa$ does not generally preclude the existence of the zero group velocity for each mode. Fig. 5 shows the eigenfunctions of the first four modes corresponding

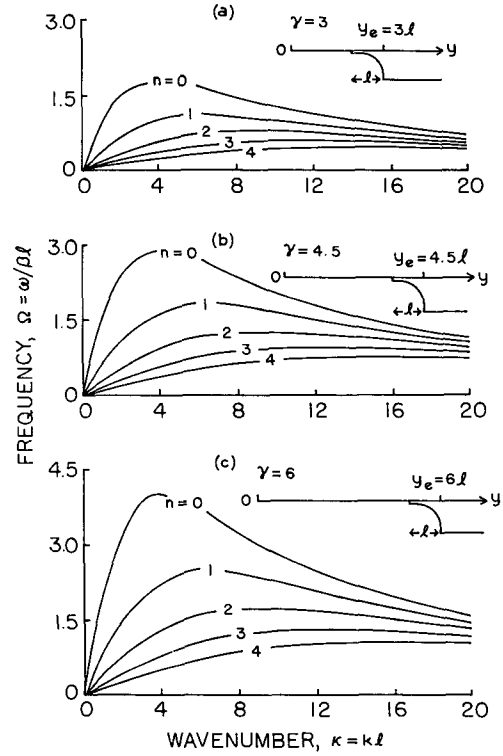

FIG. 2. As in Fig. 1 except for $B = 3$.

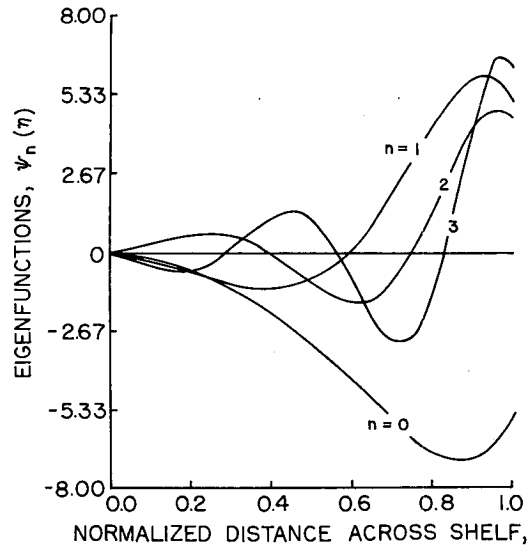

FIG. 3. The eigenfunctions ψ_n of the first four modes ($n = 0, 1, 2, 3$) computed from (5.11) (written in terms of η) for the case $B = 3$, $\gamma = 6$ and $\kappa = 5$.

to values of $\Omega_n(\kappa = 5)$ found in Fig. 4c. Qualitatively, they are similar to the eigenfunctions for case 1 (see Fig. 3). In particular, it was found that the eigenfunctions ψ_n for $n = 1, 2, 3$ did turn back at $\eta_c < 1$, in accordance with the boundary condition (3.7), which implies that ψ_n and its derivative have opposite signs at $\eta = 1$. However, at these turning points, $\psi_n(\eta_c)$ is well off the vertical scales shown.

Finally, in Fig. 6 we show that dispersion curves for $B = 3$ and values of γ so that $1/6 < \gamma < 7/6$ [(case 3), $1/2B < \gamma < 1 + 1/2B$]. Figs. 6a and 6b illustrate the interesting result that for a given B and γ pair, both positive and negative frequencies are possible, which is in agreement with the frequency bounds in (4.16). When $\gamma = 1/3$ (Fig. 6a), most of the shelf is in the Southern Hemisphere and accordingly, as this is a configuration tending toward one like case 2, apparently all but one of the eigenfrequencies are negative. The one positive eigenfrequency, labeled $n =$ "0", is very small, implying a very small phase speed.[3] When $\gamma = 2/3$ (Fig. 6b), the configuration is approaching one like case 1 and apparently all but one of the eigenfrequencies are positive. The phase speed associated with the negative root, labeled $n =$ "0" is again very small. Finally, we note that in Fig. 6c all the modes are positive, which is not unexpected since the shelf is now in the Northern Hemisphere. Fig. 7 shows the eigenfunctions for $n = 0, 1, 2$, and $n =$ "0" corresponding to the set of eigenfrequencies obtained from Fig. 6b at $\kappa = 7$. It is interesting to note that the oscillations in Fig. 7a are concentrated near the shelf break. However, the eigenfunction $\psi_{\cdots 0''}$ (Fig. 7b) becomes large at relatively small values of η and is monotonic for nearly the whole distance across the shelf.

[3] The possibility of other, smaller positive eigenfrequencies has not been ruled out; however, none was found to the numerical accuracy employed.

7. Application to Gulf of Guinea

During the coastal upwelling in 1974 Houghton and Beer (1976) observed that the sea surface temperature along the Dahomey-Ghana coast, Gulf of Guinea, exhibited periodic variations at a frequency of 0.07 cpd which propagated westward. Based on temperature data from Cotonou and

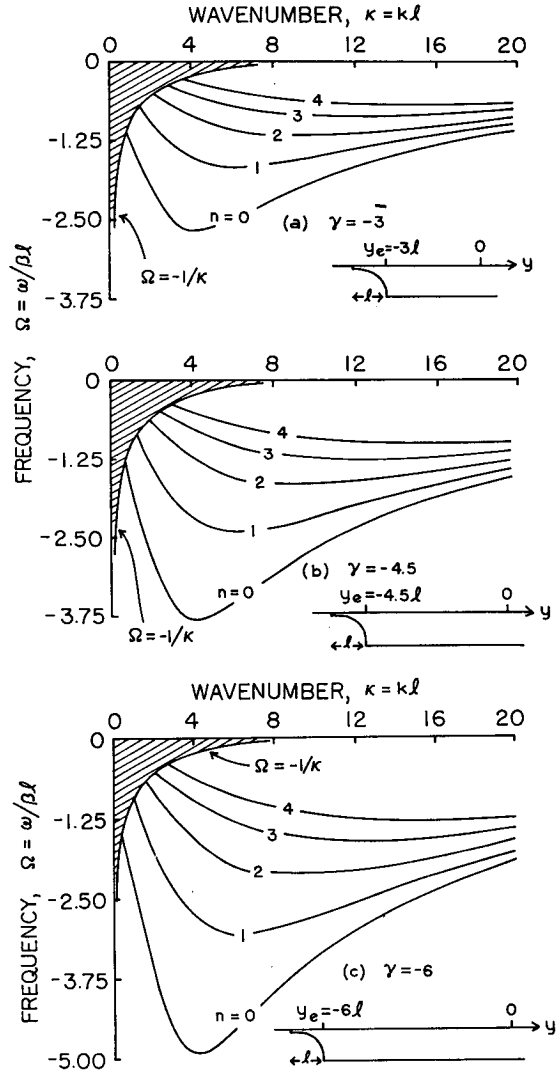

FIG. 4. The dispersion curves of the first five modes computed from (5.15) for $B = b\ell = 3$ ($b > 0$) and $\gamma = -3$, -4.5 and -6. The curve $\Omega = -1/\kappa$ represents the long-wave cutoff for trapped modes when $\Omega < 0$. These curves also apply to the cases $B = -3$ ($b < 0$) and $\gamma = 3.0$, 4.5 and 6.0 (shelf in Northern Hemisphere with deep water to the south).

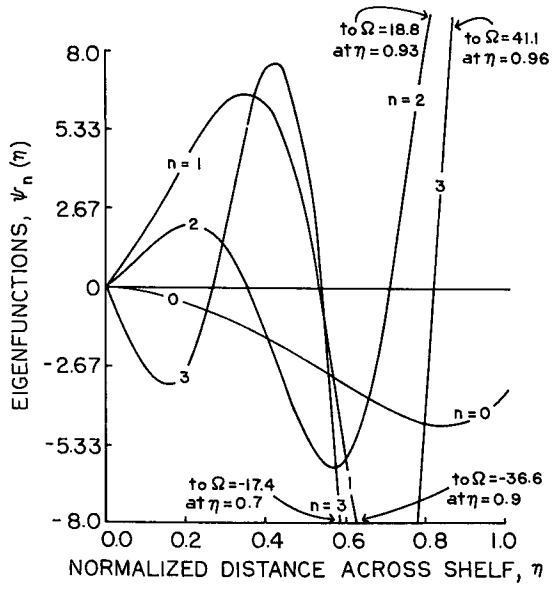

FIG. 5. The eigenfunctions ψ_n as computed from (5.16) (written in terms of η) for the case $B = 3$, $\gamma = -6$, $\kappa = 5$.

Takoradi (A and D in Fig. 8) and three other stations between these cities, they estimated the average wave (phase) speed to be 55 ± 10 km day^{-1}. Also, they observed that the wave slowed down slightly as it progressed westward. A similar westward-propagating wave of this frequency was also observed by Picaut and Verstraete, 1978) along the more extensive Dahomey-Ivory Coast. They estimated the average speed to be approximately 47 km day^{-1} and also observed that the wave slowed down as it moved westward. In particular, along the Ivory coast itself, the speed was in the range 24–28 km day^{-1}.

Houghton and Beer (1976) suggested that this wave is most likely an internal Kelvin wave, whereas Picaut and Verstraete suggested that the observed oscillation may be tidal in origin, arising out of a nonlinear interaction between the M_2 and S_2 tides in the northeast corner of the Gulf of Guinea. It is suggested here that this wave may instead be interpreted as a fundamental mode equatorial shelf wave propagating westward along an exponential shelf profile.[4] Based on the cross sections A–F shown in Fig. 9 and the shelf locations relative to the equator, γ was estimated for each section; the average of these values was found to be $\gamma = 5.85$. An average shelf width was found to be $l = 92.4$ km and an exponential profile with $B = -2.25$ was found to give a reasonable fit to all the cross sections (see Fig. 9). The dispersion curves for these values of γ and B are shown in Fig. 10. Using the value $l = 92.4$ km, we find that $\Omega = -2.4$ corresponds to the observed frequency (0.07 cpd). Careful examination of Fig. 10 reveals that there are four possible wavenumbers κ that yield a frequency of $\Omega = -2.4$. The best fit to the data is given by $\kappa = 1$ on the $n = 0$ curve, corresponding to a dimensional wavelength of 580 km. For $(\kappa,\Omega) = (1, -2.4)$, the dimensional phase speed is 40 km day^{-1}, which is just below the observed average values. The other values of κ which also give $\Omega = -2.4$ are much larger and lead to considerably smaller phase speeds. It thus appears that the observed wave may be due to a fundamental mode, nondispersive shelf wave propagating along an exponential shelf.

The eigenfunction for this mode at $\kappa = 1$ is very similar to the $n = 0$ eigenfunction shown in Fig. 5

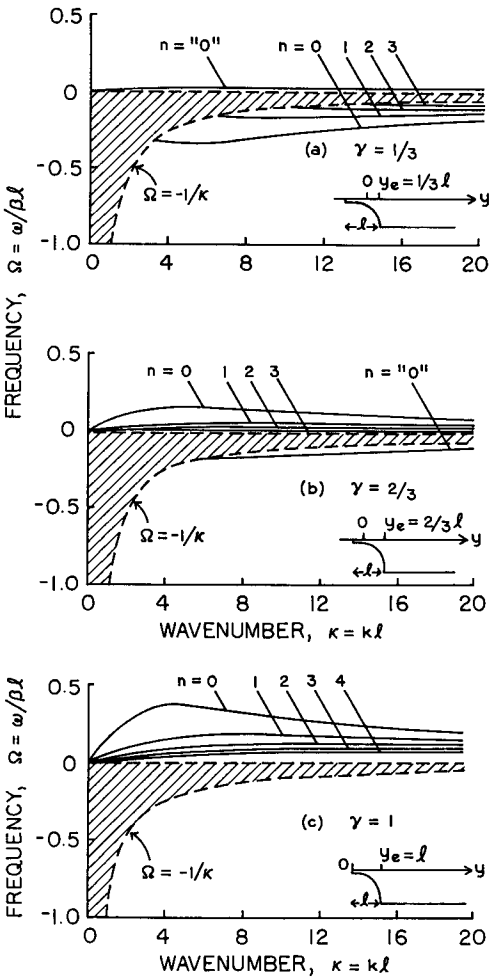

FIG. 6. The dispersion curves of the first five modes computed from (5.10) and (5.15) for $B = 3$ and three intermediate values of γ. These curves also apply to the case $B = -3(b < 0)$ and $\gamma = -1/3, -2/3, -1$ (shelf straddling equator with deep water to the south).

[4] Houghton and Beer (1976) also suggested that the wave may be a first mode shelf wave; however, the numerical computations which led them to this conclusion were not given in their paper.

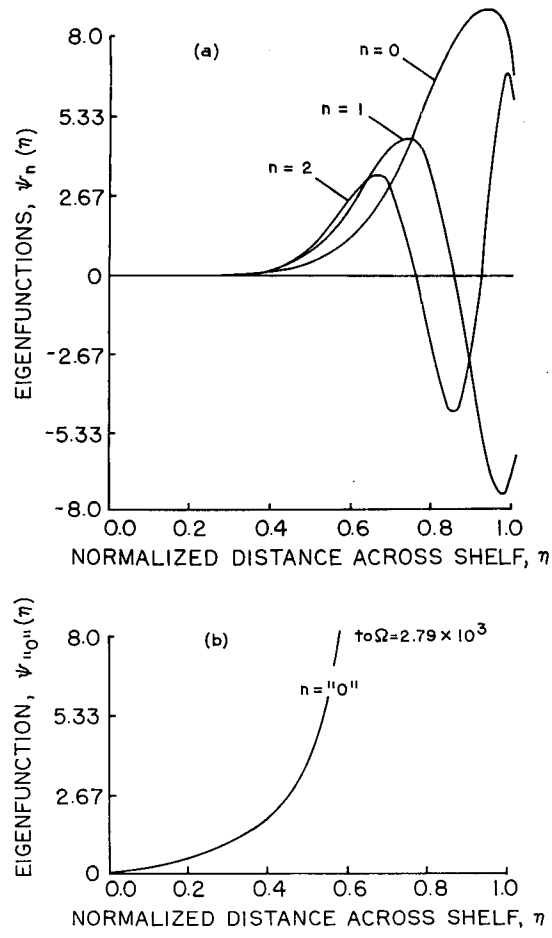

FIG. 7. The eigenfunctions of the modes $n = 0, 1, 2$ and $n =$ "0" shown in Fig. 6 for the case $B = 3$, $\gamma = 2/3$ and $\kappa = 7$.

and hence has not been reproduced here. The dispersion curves were also computed for the case $B = -2.25$ and $\gamma = 4.35$, the latter being an average value of γ for the three western stations D, E and F (see Fig. 8), which are all much closer to the equator than the three eastern stations. An average shelf width for these western stations is $l = 103$ km. In this case the theoretical speed of the fundamental mode, nondispersive wave of a frequency of 0.07 cpd was found to be 32 km day^{-1}, in good agreement with the observations. Thus we conclude that the slowing down of the wave could be mainly due to the fact that as it propagates westward it enters a shelf region which is substantially closer to the equator.

It is perhaps somewhat surprising that a barotropic model gives such good agreement with the observations, which relate to sea surface temperature fluctuations. However, the thermocline is often very

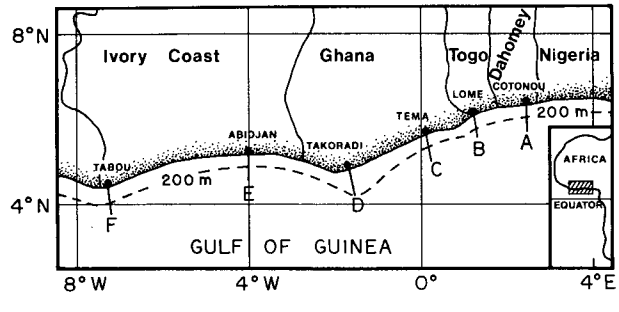

FIG. 8. The Gulf of Guinea showing the location of the 200 m depth contour. Topographic cross sections at lines A–F are plotted in Fig. 9.

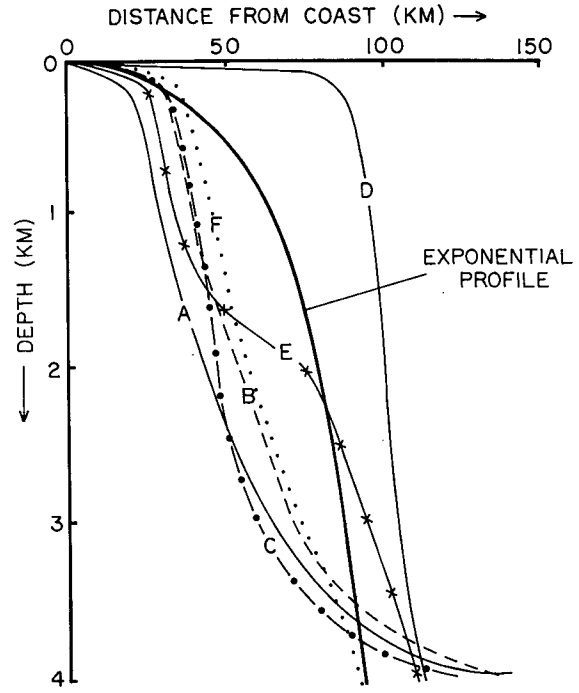

FIG. 9. Topographic cross sections at lines A–F shown in Fig. 8. The best-fit exponential profile shown corresponds to $B = -2.25$.

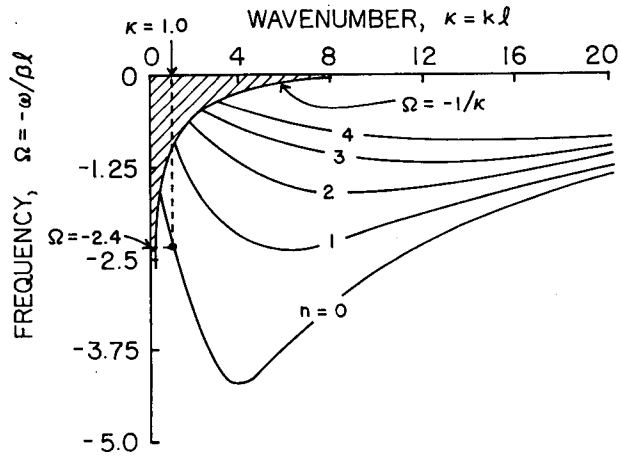

FIG. 10. The dispersion curves for the Gulf of Guinea parameters $B = -2.25$ and $\gamma = 5.85$.

shallow in the Gulf of Guinea, so that much of the shelf is essentially unstratified. It was found by Wright and Mysak (1977) that at midlatitudes, a near-surface thermocline which extends across the shelf and which is characterized by an internal deformation radius that is less than the shelf width hardly affects the speed of a barotropic shelf wave. Thus it is conceivable that the same result may also apply to barotropic equatorial shelf waves.

8. Summary

We have investigated theoretically the propagation of barotropic nondivergent trapped waves on an exponential shelf that lies parallel to the equator on an equatorial β-plane. When both the shelf and deep-sea regions are located in one hemisphere, the wave properties are very similar to those of shelf waves on a midlatitude exponential shelf located on an f-plane. Thus for each mode, the equatorial shelf wave also is nondispersive at long wavelengths, has a zero group velocity at intermediate wavelengths and in the Northern (Southern) Hemisphere the shallow water is to the right (left) of the direction of phase propagation. Further, the eigenfunctions generally have an oscillatory behavior across the shelf. When the shelf region is on one side of the equator and the deep-sea region on the other (case 2), the waves have a long-wave cutoff for trapping. However, each mode still has a zero group velocity and the above rule regarding direction of phase propagation still applies. Finally, when the shelf straddles the equator (case 3), both westward and eastward propagating modes may exist.

We have also shown that the theory may explain the presence of a long-period, westward propagating wave along the Gulf of Guinea, West Africa.

Acknowledgments. This paper was initiated while the author was visiting the National Center for Atmospheric Research (Oceanography Project) during the period February–August 1977. It is a pleasure to thank Mr. D. G. Wright for carrying out the numerical computations and for several helpful discussions. The author is also indebted to a referee for valuable comments.

REFERENCES

Abramowitz, M., and I. A. Stegun, 1965: *Handbook of Mathematical Functions*. Dover, 1046 pp.

Buchwald, T. V., and J. K. Adams, 1968: The propagation of continental shelf waves. *Proc. Roy. Soc. London*, **A305**, 235–250.

Houghton, R. W., and T. Beer, 1976: Wave propagation during the Ghana upwelling. *J. Geophys. Res.*, **81**, 4423–4429.

Mysak, L. A., 1978: Long-period equatorial topographic waves. *J. Phys. Oceanogr.*, **8**, 302–314.

Picaut, J., and J. M. Verstraete, 1978: Propagation of a 14.7-day equatorial shelf wave along the northern coast of the Guinea Gulf. Submitted to *J. Phys. Oceanogr.*

Wright, D. G., and L. A. Mysak, 1977: Coastal trapped waves, with application to the northeast Pacific ocean. *Atmosphere*, **15**, 141–150.